ITEP-6-95

Fermilab Library
0 1160 0073979 1

INSTITUTE OF THEORETICAL
AND EXPERIMENTAL PHYSICS

FERMILAB 6-95
JUL 7 199
LIBRARY

A. A. Solodsky, A. V. Stavinsky

Proton interferometry in hadron-nucleus reactions

MOSCOW 1995

UDK 539.1 M-16

PROTON INTERFEROMETRY IN HADRON-NUCLEUS REACTIONS: Preprint ITEP 6-95/

A.A.Solodsky, A.V.Stavinsky - M., 1995 - 20p.

An opportunity to determine sizes and to study shape of interaction region by interference effects in two-proton correlations at small relative momenta is discussed. Re-analysis of disposal data on the proton correlations was carried out. Results are compatible with that of more traditional approach in which the strong interaction of protons in the final state plays the main role and refine the representation about the shape of region where deep inelastic nuclear reaction takes place.

Fig. - 5, ref. - 7

© Институт теоретической и экспериментальной физики, 1995

Introduction.

A study of correlations between secondary particles at small relative momenta is powerful tool for investigation of space-time characteristics of the region of occurrence of hadron-nucleus reactions [1]. Proton correlations at small momentum difference are caused by strong interaction of protons in the final state, interference and Coulomb repulsion.

The strong interaction in the final state is the main contribution to correlations of protons at small relative momenta [2]; it provides information on the size r of the interaction region but that is indifferent to the direction of $\vec{r}$. Contribution of interference has been taken into account in the theory but didn't display explicitly. The especial interest in interference correlations is aroused from the fact that it is sensitive to the shape of the interaction region. When secondary proton source distribution has considerably not spherical symmetrical shape the interference effects caused the difference in dependencies of correlation function on different components of the relative momentum of secondaries.

Actually the nature of the correlations is determined by the average radius vector $\vec{r}$ between the secondary particles at the time beginning with which their momenta do not change substantially (for example, if rescattering is important, than after the last rescattering). The magnitude and preferred orientation of $\vec{r}$ arise not only from the size and shape of the secondary particle source itself, but also due to the movement of the secondary proton source and large time interval between emissions of protons:

$$\vec{r} \sim \vec{r}_0 + (\vec{v}_0 - \vec{v})\tau .$$

Attempts to isolate the interference contribution have been done in hA interactions [3,4]. To study the shape of the interaction region and to determine its sizes the dependencies of the correlation function $\boldsymbol{R}(\vec{q})$ on longitudinal q_l and transversal q_t components of the relative momentum $\vec{q}$ have been studied. The longitudinal size of the interaction region proved to be considerably larger than its transversal size. In this work we propose a procedure of extraction

of interference correlations, and use it to determine the size and shape of the interaction region. We re-analyze available data by applying various hypotheses about the shape of the space distribution of the secondary proton sources. Results on the sizes of the interaction region are compared with those obtained from traditional technique.

Data analysis procedure.

In accordance with the theory [2] two-proton correlation function at small relative momenta $\vec{q}$ is:

$$R(\vec{q}) \sim G(q)\cdot\left[B_i(\vec{q}) + B_f(q)\right] \qquad (1),$$

where $G(q) = \frac{2\pi\eta}{e^{2\pi\eta}-1}$ ($\eta = \alpha m_p/q$, α-the fine-structure constant) is Gamow factor of Coulomb interaction, B_i is interference contribution and B_f describes the strong final state interaction. B_f doesn't depend on the direction of $\vec{q}$ as well as the Gamow factor. Normalization of the correlation function was chosen so that $R(\vec{q}) = 1$ outside the small relative momentum region.

To isolate interference contribution in accordance with (1) we proposed to calculate the difference $D(q_1,q_2)$:

$$D(q_1,q_2) = R(q_t = q_1, q_l = q_2) - R(q_l = q_1, q_t = q_2) =$$
$$= G\left(\sqrt{q_1^2+q_2^2}\right)\cdot\left(B_i(q_t = q_1, q_l = q_2) - B_i(q_t = q_2, q_l = q_1)\right).$$

The interference contribution for two-proton correlations in the case of non-polarized protons is :

$$B_i(\vec{q}) = \frac{1}{2}\left(1 - |\tilde{\rho}(\vec{q})|^2\right) \qquad (2),$$

where $\tilde{\rho}(\vec{q})$ is Fourier transform of the source density distribution $\rho(\vec{r})$.

For comparison with experimental data the space source distribution $\rho(\vec{r})$ by orthogonal components r_x, r_y, r_z have been chosen in following forms:

(I) $$\rho(r_i) = e^{-r_i^2/2R_i^2},$$

(II) $$\rho(r_i) = \frac{1}{e^{(r_i - L_i)/\Delta} + 1}.$$

(III) $$\rho(r_i) = \begin{cases} 1 & , \text{ if } r_i < r_i^0, \\ e^{-(r_i - r_i^0)^2/2\Delta^2} & , \text{ if } r_i > r_i^0, \end{cases} \quad L_i \equiv r_i^0 + \Delta .$$

The disposal experimental data was used for construction of experimental dependence $\boldsymbol{D}_{\mathrm{Exp}}(q_1, q_2)$. This data have been fitted by curves

$$\boldsymbol{D}(q_1, q_2) = \boldsymbol{G}(q) \cdot (\boldsymbol{B}_i(q_t = q_1, q_l = q_2) - \boldsymbol{B}_i(q_t = q_2, q_l = q_1)),$$

where $\boldsymbol{B}_i$ have been taken in the sense (2). We have used in fitting the source density distributions in the form (I) for transversal components $\rho(r_x)$, $\rho(r_y)$ in all fits and the parametrizations (I), (II), (III) for longitudinal component $\rho(r_z)$. The results of fitting were the parameters R_i, L_i. Using these parameters the mean square radii for the interaction region have been obtained by the formal procedure:

$$R^{\mathrm{rms}} = \sqrt{\langle \bar{r}^2 \rangle} = \sqrt{\frac{\int_V \rho(\bar{r}) \bar{r}^2 dV}{\int_V \rho(\bar{r}) dV}} \qquad (3),$$

where V is the volume in space of $\bar{r}$.

Results.

Data of two experiments of the following type $pA \to ppX$ have been analyzed. Data [3] have been obtained in $p\mathrm{Pb} \to ppX$ reactions at $8.3 GeV/c$. Secondary protons were detected at $\theta \sim 135°(l.s.)$ with mean momentum about $0.55 GeV/c$. Data [4] have been obtained in $pA(\mathrm{C, Ti, Pb}) \to ppX$ reactions at

$7.5 GeV/c$. Secondary protons were detected at $\theta \sim 90°(l.s.)$ with mean momentum about $0.47 GeV/c$.

Following [4] we choose the longitudinal direction in the direction of $\vec{v}_0 - \vec{v}$, where $\vec{v}_0$ is velocity of the initial proton and $\vec{v}$ is velocity of the secondary protons. Such choice is natural when the point-like sources are initiated by high energy hadron along its trajectory and lifetime of the source is negligible.

When transversal components of the size related to the size of initial hadron, the form (I) for transversal components seems to be realistic; we used it in all fits. For longitudinal component r_z it is reasonable only for light nuclei. In case of heavy nucleus it is causative to suppose that the shape of longitudinal source distribution is related to Woods-Saxon distribution of nuclear density. The source distribution in form (II) reflects this fact in first approximation. To obtain the unified form which combine the features of the forms (I) and (II) we use the longitudinal source density distribution in form (III). We shall use below the term "parametrization (i)" instead of "parametrization (I) in transversal direction and (i) in longitudinal one" for brevity.

The fixed value for parameter $\Delta = 1 fm$ was chosen. There are some reasons to choose the value of the parameter Δ larger than standard value of width parameter for Woods-Saxon distribution (due to impact parameter distribution) and smaller (because of protons in [3,4] are cumulative particles and could be produced only by dense fluctuation of nuclear matter). The statistical errors of available data aren't enough to consider Δ as a free parameter.

By parametrizations (I) and (III) the data for all nuclei-targets were fit. The results of these fits are shown in figures 1.I, 2.I, 3.I, 4.I and 1.III, 2.III, 3.III, 4.III accordingly. The parametrization (II) was used only with respect to heavy nuclear (Pb) and results of these fits are shown in figures 1.II, 2.II . Each figure shows: a). The source density distribution $\rho(\vec{r})$ in components $\rho(r_x) = \rho(r_y)$ and $\rho(r_z)$; b). Fourier transforms $\tilde{\rho}(q_x) = \tilde{\rho}(q_y)$ and $\tilde{\rho}(q_z)$; c). The experimental dependence $D(q_1, q_2)$ with calculated curve for chosen values of

parameters and d). The best parameters of fitting by the χ^2 criterion and contours of the 67% and 98% confidence levels. The fitted parameters for the parametrizations (I), (II) and (III) are listed in tables I, II, III correspondingly.

Table I.

Notes	χ^2/DoF	$R_x = R_y (fm)$	$R_z = R_z^{rms} (fm)$
Pb, 90°	7.9/10	$1.9^{+0.5}_{-0.4}$	$4.4^{+1.9}_{-1.2}$
Pb,135°	9.7/5	0.01+1.2	$4.6^{+1.5}_{-1.3}$
Ti, 90°	2.5/7	$1.5^{+0.5}_{-0.7}$	$4.0^{+1.3}_{-2.1}$
C, 90°	3.3/7	$1.1^{+0.6}_{-1.1}$	$3.2^{+1.7}_{-1.2}$

Table II.

Notes	χ^2/DoF	$R_x = R_y (fm)$	$L_z (fm)$	$L_z^{rms} (fm)$
Pb, 90°	6.7/10	$2.1^{+0.6}_{-0.5}$	$7.2^{+1.9}_{-1.6}$	$4.5^{+1.0}_{-0.8}$
Pb,135°	7.9/5	0.01+1.3	7.9±1.8	$4.9^{+1.0}_{-0.9}$

Table III.

Notes	χ^2/DoF	$R_x = R_y (fm)$	$L_z (fm)$	$L_z^{rms} (fm)$
Pb, 90°	6.2/10	$2.3^{+0.7}_{-0.6}$	$7.0^{+1.5}_{-1.2}$	$4.2^{+0.8}_{-0.7}$
Pb,135°	7.1/5	0.01+1.3	7.9±1.5	4.8±0.8
Ti, 90°	1.9/7	$2.0^{+0.7}_{-0.4}$	$4.7^{+1.2}_{-1.1}$	$3.0^{+0.7}_{-0.6}$
C, 90°	2.0/7	$1.2^{+0.8}_{-1.2}$	$5.3^{+1.0}_{-1.2}$	$3.3^{+0.6}_{-0.7}$

Within statistical errors all three parametrizations are in agreement with the experimental data. To obtain qualitative visualization about difference of two parametrizations Gaussian and parametrization (III) (the result of which most different) both

curves for Pb ($\bar{\theta} = 135°$) are shown in fig.(5). From this figure one can see that the experimental data state about presence of the narrow deep where as Gaussian parametrization as distinct from the parametrization (III) doesn't realize it in sufficient degree.

From the tables I, II, III one can see that:

a) longitudinal sizes more than transversal; longitudinal-transversal ratio is about $1.5 \div 3$ for $\bar{\theta} = 90°$ and more than 4 for $\bar{\theta} = 135°$. As it was mentioned above the experiment [3] and [4] differ each from other not only in mean polar angle of secondary protons but also in its mean momentum $\bar{p}$.

b) both longitudinal and transversal sizes show tendency to growth with increasing of A .

The longitudinal and transversal sizes have been used to calculate the values R^{rms} in accordance with [3,4]. The results of calculations are shown in table IV. Available data are also shown for comparison. The indicated errors are statistical.

Table IV.

Notes	$R_I^{rms}(fm)$	$R_{II}^{rms}(fm)$	$R_{III}^{rms}(fm)$	$R_a^{rms}(fm)$	$R_b^{rms}(fm)$
Pb, 90°	$4.8^{+1.6}_{-1.1}$	$5.0^{+0.8}_{-0.7}$	$4.8^{+0.7}_{-0.5}$	$5.01 \pm .30$	$5.42 \pm .14$
Pb, 135°	$4.6^{+1.5}_{-1.3}$	$4.9^{+1.0}_{-0.9}$	4.8 ± 0.8	—	$6.25 \pm .70$
Ti, 90°	$4.3^{+1.1}_{-2.0}$	—	$3.6^{+0.5}_{-0.6}$	$4.14^{+0.28}_{-0.24}$	$4.34 \pm .16$
C, 90°	$3.3^{+0.9}_{-1.0}$	—	$3.5^{+0.3}_{-0.5}$	$3.05 \pm .21$	$3.02 \pm .11$

When our results on R^{rms} are compared with that from [3,4] one should have in mind one circumstance. In [3,4] R^{rms} was extracted mainly from the value of narrow peak at $q \sim 40\, MeV/c$. Our procedure explore the interval $q \sim 150\, MeV/c$. The mean momentum of secondaries correlates to the value of q: in [4] the mean momentum of protons for the small q region was $0.41 GeV/c$ while the mean momentum for all protons in this experiment was $0.47 GeV/c$ [5]. Having in mind the dependence of $R^{rms}(\bar{p})$ [4]

one should compare our new results with data at $\bar{p} = 0.47 GeV/c$ More correct comparison is possible for [4] where data for different momenta of secondaries are presented. The values of R^{rms} for $\bar{p} = 0.475 GeV/c$ are listed in the fourth column of the table IV and the data for full momentum range of secondary protons are listed in last column.

Having in mind previous discussion one can say that the values of R^{rms} have been extracted from interference are in a good agreement with previous data.

We would like to compare our results on L_z (parametrization (III) for definition; it is shown in last column of the table V) with simple estimations. We used for estimation $R_A = 1.4\sqrt[3]{A}\, fm$ The mean values of the length of trajectory inside the sphere with radii R_A is $\bar{l}_0 = 4/3\, R_A$ ($\bar{l}_0/2$ is presented in second column of the table V)

Table V.

Notes	R_A (fm)	$\bar{l}_0/2$ (fm)	$\bar{l}_0F/2$ (fm)	$\bar{l}_0Fk/2$ (fm)	L_z (fm)
Pb, 90°	8.3	5.5	6.1	8.1	$7.0^{+1.5}_{-1.2}$
Pb, 135°	8.3	5.5	7.8	10.4	7.9 ± 1.5
Ti, 90°	5.1	3.4	3.7	5.0	$4.7^{+1.2}_{-1.1}$
C, 90°	3.2	2.14	2.4	3.1	$5.3^{+1.0}_{-1.2}$

In [6] possible correlations between the point and the moment of secondary particle emission in hA interactions was taken into account; angular dependence of measuring size was proposed in following form :

$$l \sim l_0\sqrt{\sin^2\theta + \left(\frac{v}{v_0} - \cos\theta\right)^2} \equiv l_0 F \qquad (5).$$

The value of $\bar{l}_0F/2$ is shown in third column of table V. The impact parameter distribution for inelastic interaction with two-proton emission is shifted into its small values with respect to

distribution for all interactions. Due to this reason the value of $\bar{l}$ could be larger by factor $9/8 \div 4/3$ [7]. The value of $\bar{l}_0 Fk/2$ (where $k = 4/3$) is shown in fourth column. One can see from the table V that values in fourth column are close to experimental results. It's state that cumulative particles are emitting mainly from central collisions.

Conclusions.

For the first time the sizes of emitting region for protons were obtained on the basis of interference consideration.

The mean sizes are in accordance with that obtained by traditional technique. The equality of sizes of the interaction region extracted from interferometry contribution and from superposition of all contributions (when interferometry is not dominant part) is important test of validity of the approach in which small angle correlations are used to study the space-time characteristics of the source.

It was found that shape of the source is non-spherical for *hA* interaction: the longitudinal components of the size is larger then the transversal components. For heavy nuclei the form of parametrization (III) is preferable in longitudinal direction but all types of parametrization are acceptable within statistical errors. Data show that cumulative particles are emitting mainly from central collisions.

The authors are grateful to G.A.Leksin and E.A.Doroshkevich for helpful discussions and valuable remarks.

Pb, $\bar{\theta} = 90°$

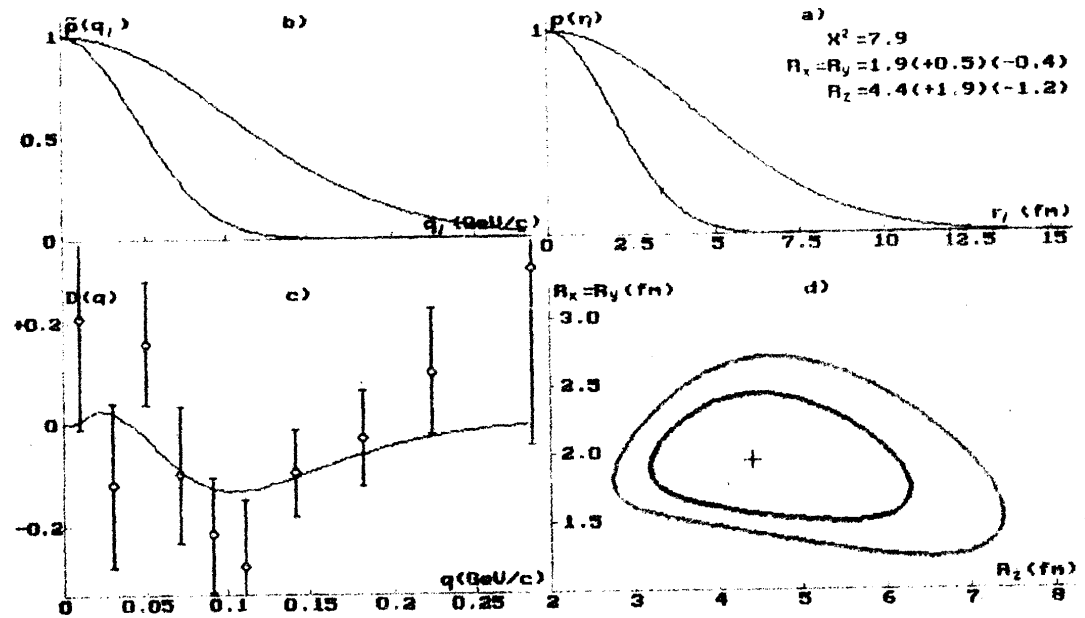

Fig. 1.I

Pb, $\bar{\theta} = 135^\circ$

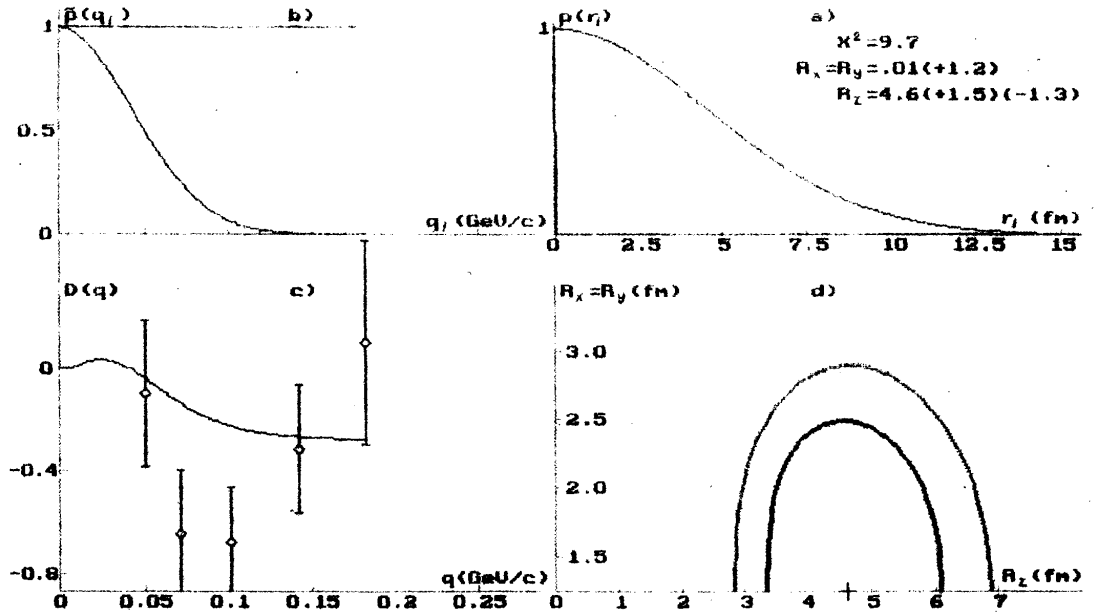

Fig. 2.I

Ti, $\bar{\theta} = 90°$

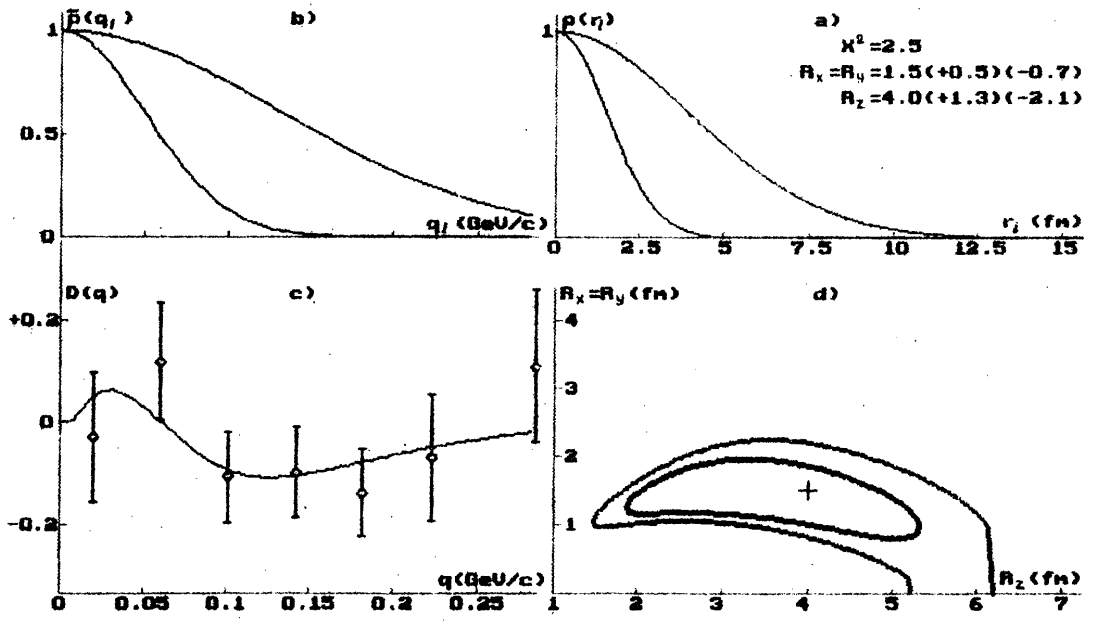

Fig. 3.I

C, $\bar{\theta} = 90°$

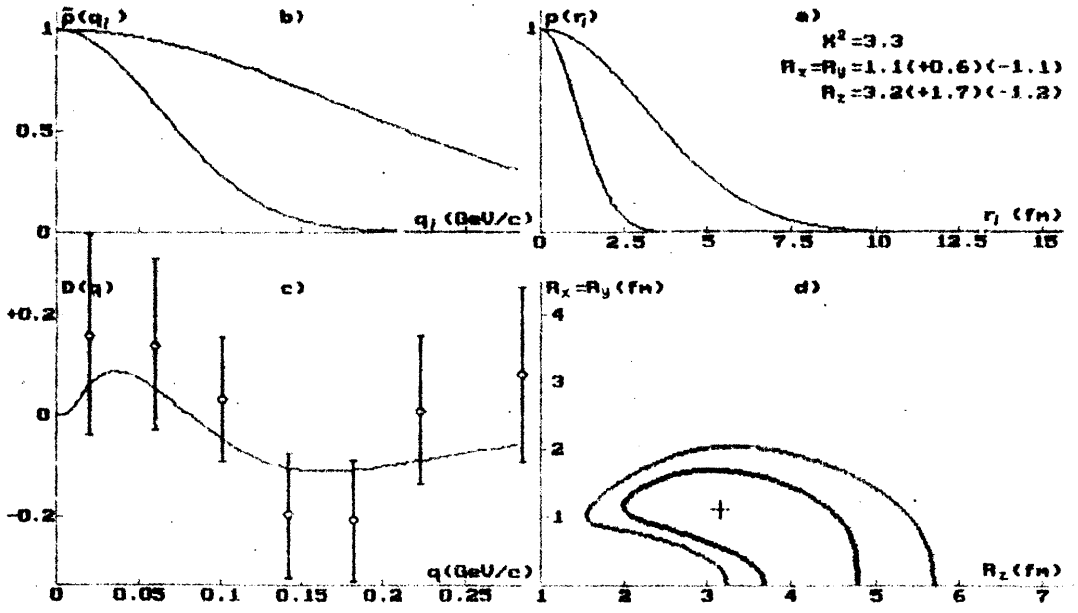

Fig. 4.I

Pb, $\bar{\theta} = 90°$

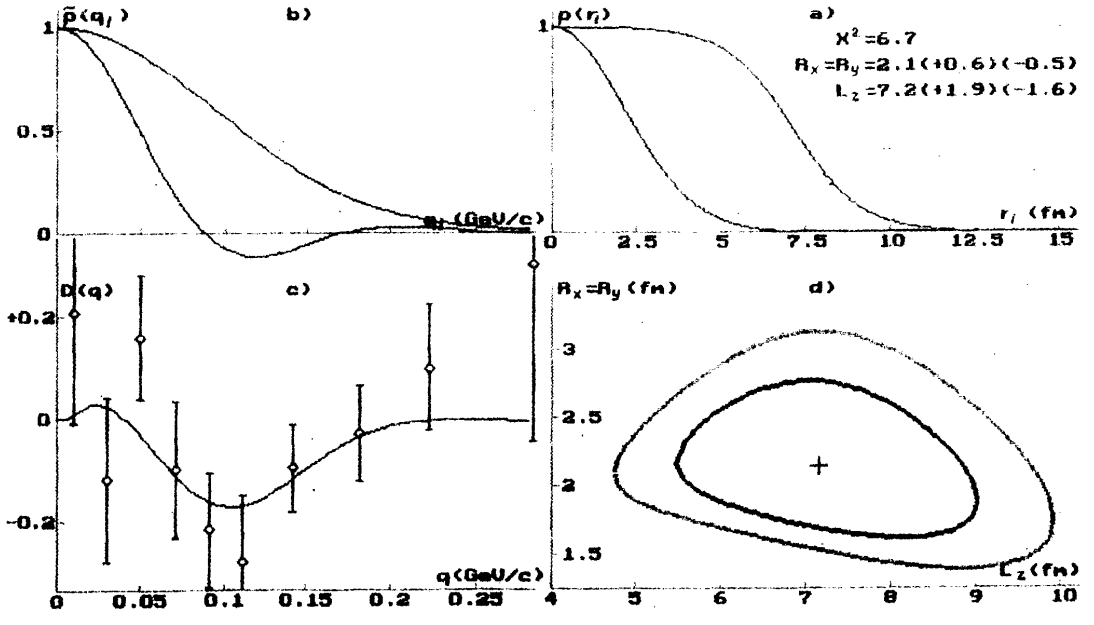

Fig. 1.II

Pb, $\bar{\theta} = 135°$

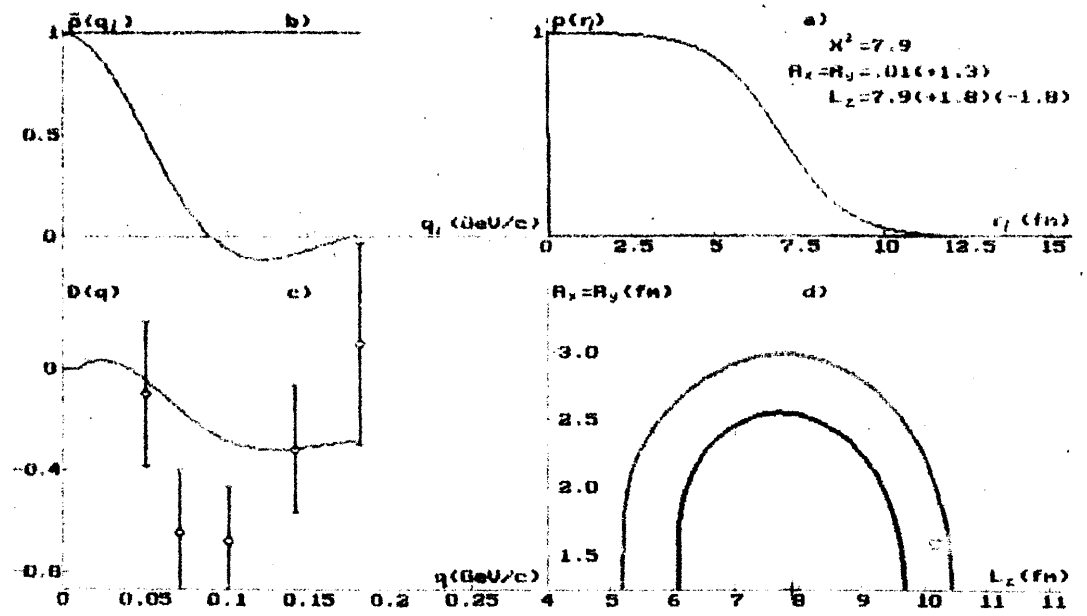

Fig. 2.II

Pb, $\bar{\theta} = 90°$

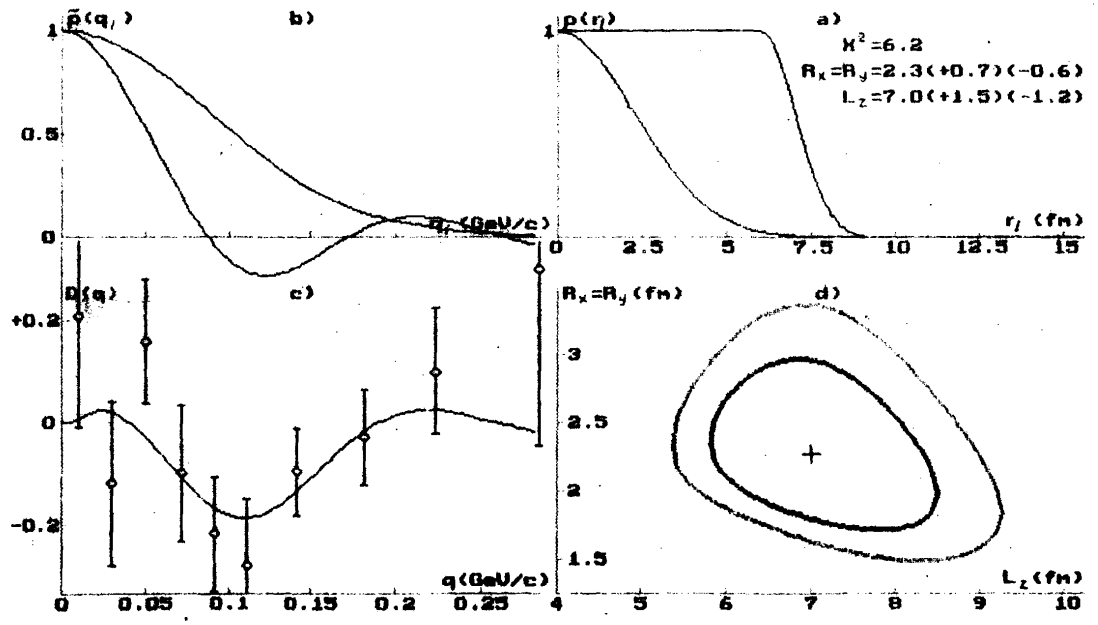

Fig. 1.III

Pb, $\bar{\theta} = 135°$

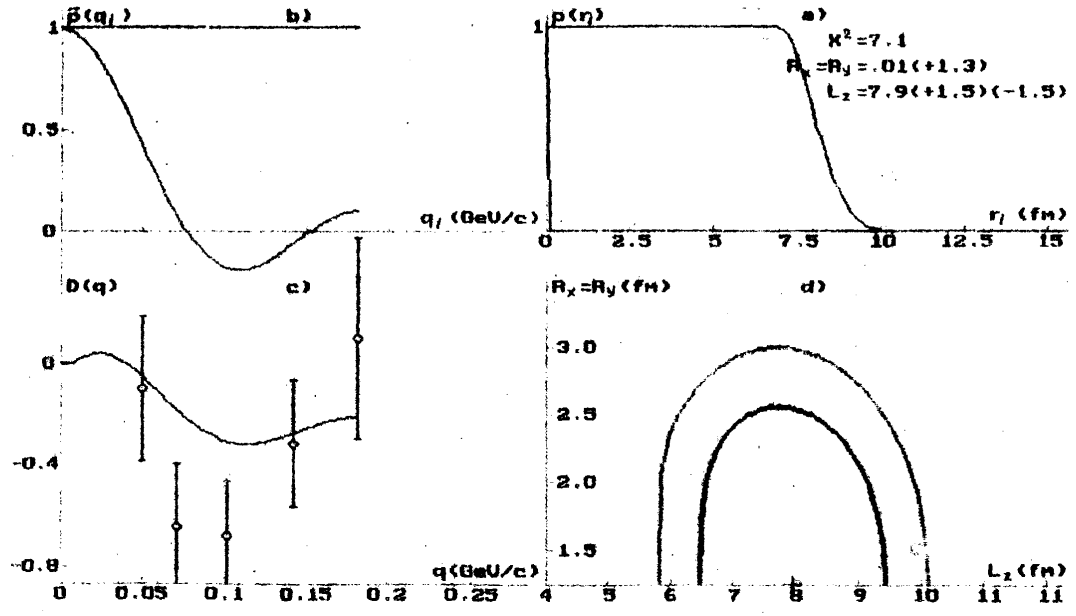

Fig. 2.III

Ti, $\bar{\theta} = 90°$

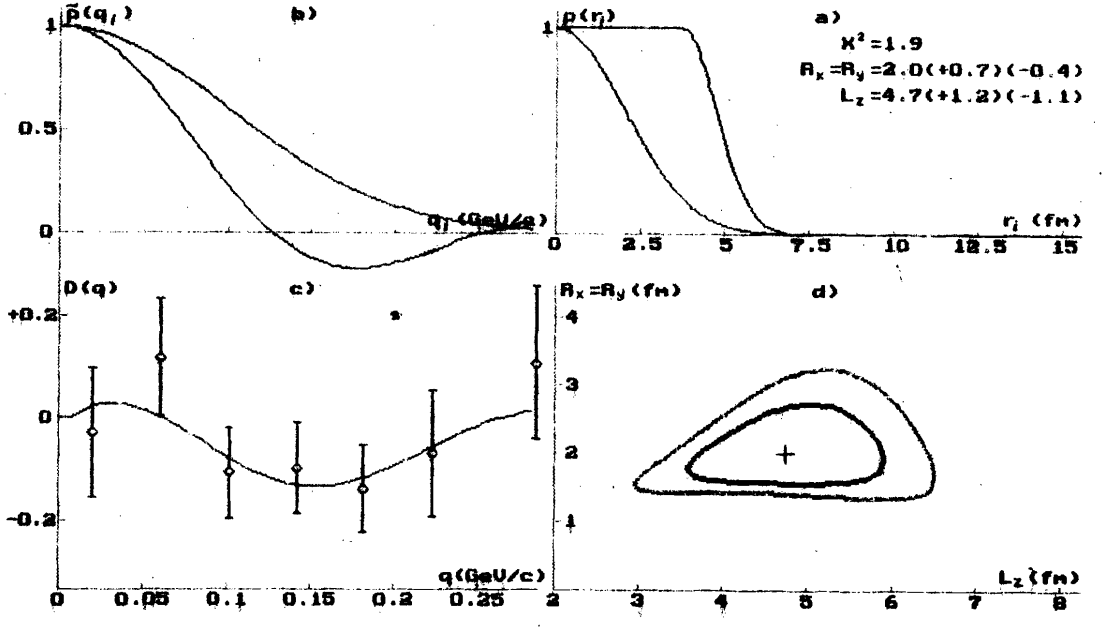

Fig. 3.III

C, $\bar{\theta} = 90°$

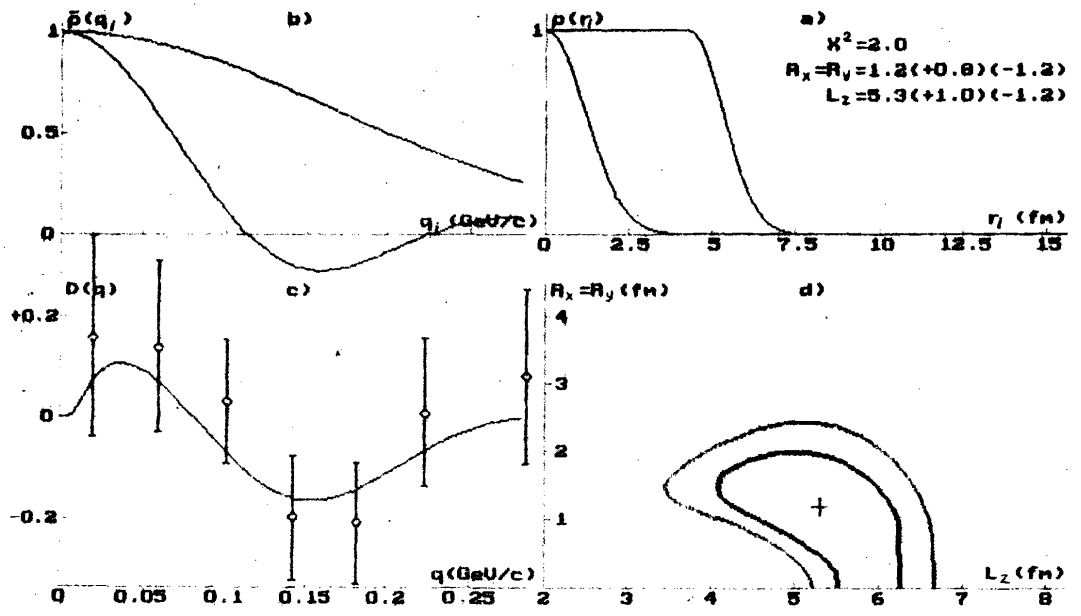

Fig. 4.III

Pb, $\bar{\theta} = 135°$

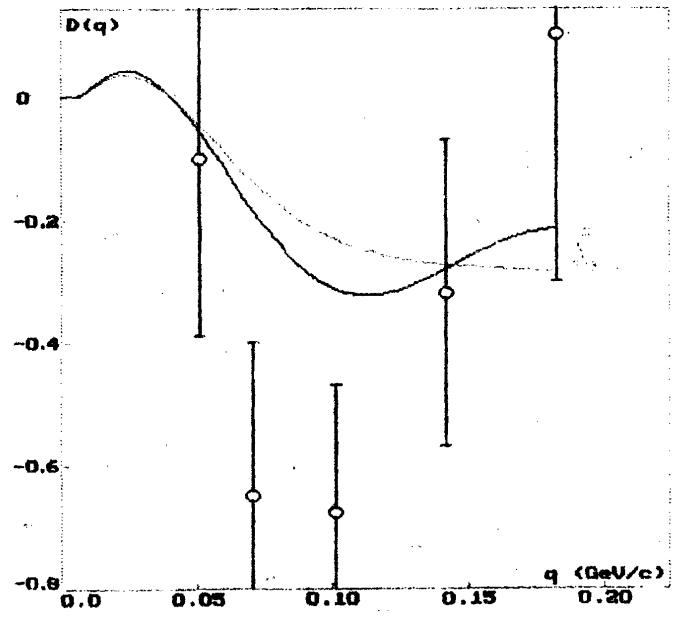

Fig. 5

Picture captions.

Fig.1.I

For Pb ($\bar{\theta} = 90°$) in case of parametrization (I): a).The source density distribution $\rho(\bar{r})$ in components $\rho(r_x) = \rho(r_y)$ and $\rho(r_z)$; b). Fourier transforms $\tilde{\rho}(q_x) = \tilde{\rho}(q_y)$ and $\tilde{\rho}(q_z)$; c). The experimental dependence $D(q_1, q_2)$ with calculated curve for chosen values of parameters and d). The best parameters of fitting by the χ^2 criterion and contours of the 67% and 98% confidence levels.

Fig.2.I

The same as in fig.1.I for Pb ($\bar{\theta} = 135°$).

Fig.3.I

The same as in fig.1.I for Ti ($\bar{\theta} = 90°$).

Fig.4.I

The same as in fig.1.I for C ($\bar{\theta} = 90°$).

Fig.1.II

The same as in fig.1.I in case of parametrization (II).

Fig.2.II

The same as in fig.2.I in case of parametrization (II).

Fig.1.III

The same as in fig.1.I in case of parametrization (III).

Fig.2.III

The same as in fig.2.I in case of parametrization (III).

Fig.3.III

The same as in fig.3.I in case of parametrization (III).

Fig.4.III

The same as in fig.4.I in case of parametrization (III).

Fig.5

The experimental dependence $D(q_1, q_2)$ with calculated curves in case of parametrizations (I) and (III) for Pb ($\bar{\theta} = 135°$).

References.

[1] G.I.Kopylov and M.I.Podgoretsky, *Sov.J.Nucl.Phys.* **15**, 219 (1972)
S.E.Koonin, *Phys.Lett.* **70B**, 43 (1977)

[2] R.Lednicky and V.L.Lyuboshits, *Sov.J.Nucl.Phys.* **35**, 770 (1982)

[3] A.V.Vlassov *et.al.*, *Sov.J.Nucl.Phys.* **36**, 536 (1982)

[4] Yu.D.Bayukov *et.al.*, *Sov.J.Nucl.Phys.* **50**, 638 (1989)

[5] Yu.D.Bayukov *et.al.*, *Sov.J.Nucl.Phys.* **50**, 447(1989)

[6] V.B.Gavrilov *et.al.*, *Sov.J.Nucl.Phys.* **41**, 540 (1985)

[7] A.V.Vlassov *et.al.*, *Sov.J.Nucl.Phys.* **58**(4) (1995)
A.V.Vlassov *et.al.*,*Preprint ITEP* **57** (1990)

А.А.Солодский и др.

Протонная интерферометрия в адрон-ядерных реакциях.

Подписано к печати 17.02.96 Формат 60x90 1/16 Офсетн.печ.
Усл.-печ.л.1,25 Уч.-изд.л.0,9 Тираж 124 экз. Заказ 6.
Индекс 3649

Отпечатано в ИТЭФ, 117259, Москва, Б.Черемушкинская,25